Nuclear Instruments and Methods in Physics Research A 619 (2010) 115–118

Contents lists available at ScienceDirect

Nuclear Instruments and Methods in Physics Research A

journal homepage: www.elsevier.com/locate/nima

Effect of metal ion on the structure and function of *Li*PDF: The study of the fine structure around the metal site using XANES

Yu Wang [a,b], Wangsheng Chu [a,*], Feifei Yang [a], Meijuan Yu [a], Haifeng Zhao [a], Weimin Gong [c], Yuhui Dong [a], Yaning Xie [a], Ziyu Wu [b,a,**]

[a] Institute of High Energy Physics, Chinese Academy of Sciences, Beijing 100049, China
[b] National Synchrotron Radiation Laboratory, University of Science and Technology of China, Hefei 230029, China
[c] National Laboratory of Biomacromolecules, Institute of Biophysics, Chinese Academy of Sciences, Beijing 100101, China

ARTICLE INFO

Available online 18 February 2010

Keywords:
*Li*PDF
BioXAS
Metalloprotein

ABSTRACT

We used X-ray absorption near edge structure (XANES) spectroscopy to investigate the metal-dependent enzymatic activity of the peptide deformylase from *Leptospira interrogans* (*Li*PDF). *Ab initio* full multiple scattering calculations performed by MXAN are applied to obtain the local structure of the cobalt-containing *Li*PDF (Co-*Li*PDF) and zinc-containing *Li*PDF (Zn-*Li*PDF) around the metal sites in pH9.0 buffer solution. The result shows the cobalt-wat1 (the bond water molecule) distance of Co-*Li*PDF is 1.89 Å, much shorter than that of Zn-*Li*PDF, 2.50 Å. That is an essential factor for its low catalytic activity.

1. Introduction

Peptide deformylase (PDF, EC 3.5.1.27) is an important member of the zinc metalloproteases superfamily. In eubacterium, as well as in mitochondria and chloroplasts, the protein synthesis starts from formylmethionine-tRNA$_i$, resulting in the synthesis of N-terminally formylated polypeptides [1]. During the elongation of the polypeptide chain the formyl group is removed hydrolytically by the PDF enzyme [2–4], which may be a universally conserved feature of the prokaryotic protein synthesis and an essential component for bacterial survival [5]. Actually there is an increasing demand from new effective drugs because of the continuous increase of tolerance problems occurring with conventional antibiotics. PDF is an attractive target for the design of new antibiotics because deformylation apparently does not occur in the cytoplasm of eucaryotic cells [6].

Previous work has shown that the catalytic efficiency of PDFs strongly depend on the identity of the bound metal. *Escherichia coli* PDF(*Ec*PDF) containing Zn^{2+} is much less active than that containing Fe^{2+},Ni^{2+} and Co^{2+}, while for *Leptospira interrogans* PDF (*Li*PDF) ,that containing Zn^{2+} is more active than others [7–9]. Little is known about the chemical and physical mechanisms responsible for the enzymatic activity difference of *Li*PDFs due to the lack of the fine structure around the metal sites in these proteins.

X-ray absorption spectroscopy (XAS) is a unique tool to probe the local structure of metalloproteins around metal sites at atomic-level resolution [10–15], where biological samples can be studied in a variety of forms, including oriented single protein crystals, unoriented microcrystals, frozen or room-temperature solutions and proteins inserted in membranes. Here, we measured the Zn and Co *K*-edge XAS spectra for zinc-containing *Li*PDF(Zn-*Li*PDF) and cobalt-containing *Li*PDF (Co-*Li*PDF), respectively, in pH 9.0 buffer solution. Combining *ab initio* multiple scattering calculation, we extracted the subtle local structure information around metal sites for both *Li*PDF proteins, especially the position of the bond water molecule.

2. Materials and methods

E.coli BL21(DE3) cells carrying plasmid pET22b-*Li*PDF were expressed as previously reported [7]. Cells were harvested by centrifugation, and resuspended in 25 ml of buffer A (50 mM Tris-HCl7.5, 10 mM NaCl). After sonication cell debris was removed by centrifugation. The supernatant (25 ml) was applied onto a HiTrapTM 5 ml Q HP (Amersham Pharmacia Biotech) column equilibrated with buffer B (50 mM Tris-HCl pH 8.5, 10 mM NaCl). The column was eluted with 250 ml of buffer B plus a linear gradient of 10 mM–1 M NaCl (AKTA purifier 900, Amersham Pharmacia Biotech). The fractions with PDF activity were concentrated and applied to a SuperdexTM 75 column (16/60, Amersham Pharmacia Biotech) pre-equilibrated with buffer C (50 mM Tris-HCl pH 8.5, 50 mM NaCl). The fractions containing *Li*PDF activity were collected. The sample homogeneity was monitored by SDS-PAGE and the protein concentration was determined by Braford assay with BSA as the standard. Finally,

* Corresponding author at: Institute of High Energy Physics, Chinese Academy of Sciences, Beijing 100049, China.
** Corresponding author at: National Synchrotron Radiation Laboratory, University of Science and Technology of China, Hefei 230029, China.
E-mail addresses: cws@ihep.ac.cn (W. Chu), wuzy@ustc.edu.cn (Z. Wu).

0168-9002/$ - see front matter © 2010 Elsevier B.V. All rights reserved.
doi:10.1016/j.nima.2010.02.093

the purified protein was dialyzed against 50 mM NaH_2PO_4/Na_2HPO_4 (pH 9.0) and concentrated to about 60 mg/ml. The Zn^{2+} concentration is about 200 ppm. The enzymatic activity of Zn-*Li*PDF is nearly constant from pH 7.5–10.5 [7]. We choose pH 9.0 just as it is in the middle of the active range.

Samples of Co-*Li*PDF were prepared by incubation of metal-free *Li*PDF. Metal-free *Li*PDF was prepared by adding 15 ml of 0.1 M EDTA to 0.5 ml of 60 mg/ml protein for 2 hours at 277 K. There was no Zn element left as monitored by X-ray fluorescence method. The additional EDTA was then removed by direct exchange dialysis and concentrated in centrifugal tube. The procedure was repeated twice by direct exchange dialysis (dilute 100×100 times) and concentrated in centrifugal tube (dilute 15×15 times). Metal-free *Li*PDF (0.5 ml, 20 mg/ml) was incubated with 1.2 mM $CoCl_2$ 60 ml for 2 hours at 277 K and then concentrated to 20 mg/ml. The purified Co-*Li*PDF was dialyzed against 50 mM NaH_2PO_4/Na_2HPO_4 (pH 9.0) and afterwards concentrated to 30 mg/ml. The Co^{2+} concentration is about 100 ppm. The sample homogeneity was monitored by SDS-PAGE. The protein concentration was finally determined by Braford assay with BSA as the standard [16].

Measurements of the Zn *K*-edge and Co *K*-edge were carried out at the beam line 4W1B of the Beijing Synchrotron Radiation Facility (BSRF, China) in the fluorescence yield (FY) mode at room temperature. The typical energy of the storage ring was 2.5 GeV and experiments were performed with a decreasing electron current from 250 to 160 mA. The incident beam intensity was monitored using an ionization chamber flooded by a 25% argon-doped nitrogen mixture while the fluorescence signal was collected by means of a Lytle detector flooded by argon gas.

In order to extract the structural/geometrical information around the metal site, we performed a quantitative analysis of the XANES spectrum using the MXAN code [17,18]. This code is capable of performing a quantitative analysis of a XANES spectrum from the absorption edge up to 200 eV via comparison between experimental data and many theoretical calculations obtained by changing relevant geometrical parameters of the atomic site [19–21]. The X-ray absorption cross-sections are calculated using the full multiple scattering scheme in the framework of the muffin-tin (MT) approximation for the shape of the potential [22,23]. In this case, the exchange and correlation part of the potential have been determined on the basis of the local density approximation of the self energy. Inelastic processes have been taken into account by a convolution with a broadening Lorentzian function having an energy-dependent width of the form $\Gamma(E)=\Gamma_c+\Gamma_{mfp}(E)$. The constant part Γ_c includes the core-hole lifetime (1.8 eV) [24] and the experimental resolution (1.5 eV), while the energy-dependent term represents all the intrinsic and extrinsic inelastic processes [21,25,26]. The muffin-tin radii were chosen according to the Nofrman criterion with a 15% overlap [27,28]. This method takes into account, for Multiple-Scattering events, a rigorous way through the evaluation of the scattering path operator [22,29] and its effectiveness has been successfully tested over the years in a number of different applications [19,25]. The spectrum is convergent when the cluster includes 39 atoms within a radius of 5.5 Å. Therefore the local structure of the *Li*PDF active center can be properly represented by a cluster that contains all the 50 atoms within 6 Å from zinc ion.

3. Results and discussion

The Zn *K*-edge XANES spectrum of Zn-*Li*PDF (red curve) and the Co *K*-edge XANES spectrum of Co-*Li*PDF in buffer solution at pH 9.0 are shown in Fig. 1. Here the zero energy corresponds to

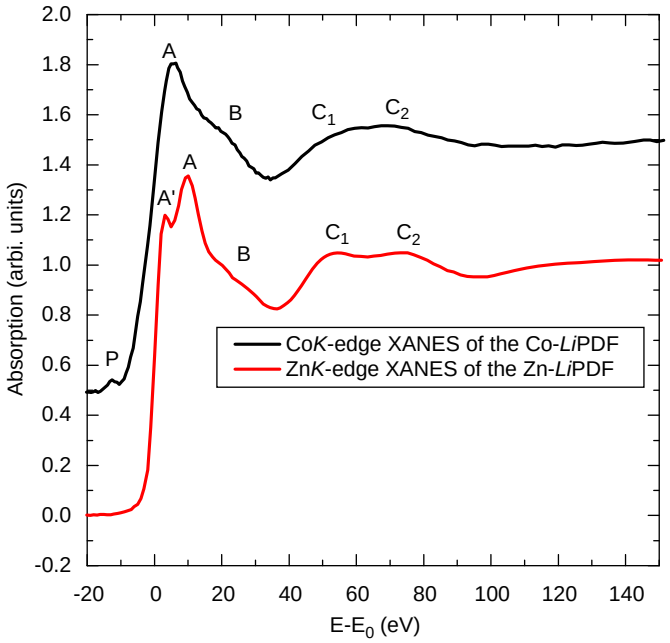

Fig. 1. Zn *K*-edge XANES spectrum of Zn-*Li*PDF (red curve) and Co *K*-edge XANES spectrum of Co-*Li*PDF in buffer solution at pH 9.0. (For interpretation of the references to color in this figure legend, the reader is referred to the web version of this article.)

the absorption edge of the two spectra. It can be seen that both of the XANES spectra present the similar features above 20 eV. As we know, the XAS feature of this region is mainly dominated by the scattering events of the neighbor atoms around the absorbed atom, but not sensitive to the electronic structure of metals. It indicates Co^{2+} and Zn^{2+} locate the similar chemical environment in the *Li*PDF proteins. However, the subtle change of the two XANES spectra also exists, especially for the peaks C_1 and C_2, indicating the fine local structure changes when Co^{2+} substitutes Zn^{2+}. Here it should be noted that the big difference present in the region -10 to 20 eV is due to the different 3d electronic configuration of metals. An obvious pre-edge peak can be observed in the XANES spectrum of the Co-*Li*PDF, because of the unoccupied 3d orbital. The peak A is due to the scattering among the nearest neighbors and it can reflect not only the geometric structure but also the electronic structure. Due to the electronic configure of the Zn^{2+} is different from that of Co^{2+}, so we can not directly compare the main peak A in the spectrum of Co-*Li*PDF with that of Zn-*Li*PDF.

In order to obtain the exact structural information around the metal site, we performed a quantitative analysis of the XANES spectrum using the MXAN code, based on the crystallographic structure of *Li*PDF (PDB code 1Y6H(B)) [30,31]. Fig. 2 shows the best fits (blue dots) of the experimental XANES spectra (red curve) of Zn-*Li*PDF (left) and Co-*Li*PDF (right) in buffer solution at pH 9.0. As we can see, all features in the near-edge region of the XANES spectra at the Zn and Co *K*-edge have been successfully reproduced. The square residue values for these calculations are 0.45 and 0.87, respectively. Some refined critical distances of the best fits are summarized in Table 1. The comparison of the local structure obtained by the best fits for the Zn-*Li*PDF and the Co-*Li*PDF is plotted in Fig. 3.

Our result shows the most important difference of the local structure around center metal between Co-*Li*PDF and Zn-*Li*PDF is the position of the wat1. The cobalt-wat1 distance of Co-*Li*PDF is 1.89 Å, much shorter that of Zn-*Li*PDF, 2.50 Å. In most of PDF proteins and PDF complexes, the length of the metal-wat1 bond

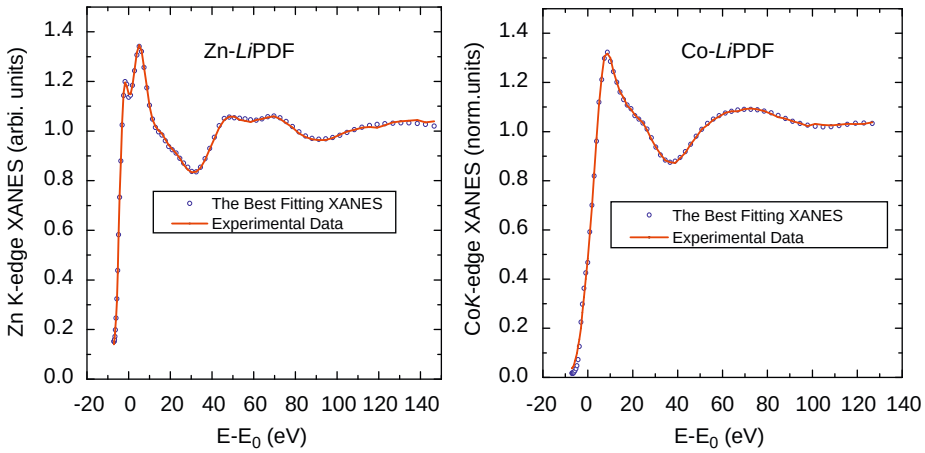

Fig. 2. Best fit of the XANES spectra (blue dots) of Zn-*Li*PDF (left) and Co-*Li*PDF (right) in buffer solution at pH9.0, compared with experimental spectra (red line). (For interpretation of the references to color in this figure legend, the reader is referred to the web version of this article.)

Table 1
Refined critical distances of Zn-*Li*PDF and Co-*Li*PDF.

Atom pairs	Model structure distance (Å)	Zn-*Li*PDF fitting distance (Å)	Co-*Li*PDF fitting distance (Å)
S^2 (square residue)	–	0.45	0.87
Metal His147-(NE2)	2.15	2.03 ± 0.02	2.03 ± 0.03
Metal His143-(NE2)	2.17	2.04 ± 0.02	1.85 ± 0.02
Metal Cys101-(SG)	2.40	2.23 ± 0.02	2.32 ± 0.03
Metal Wat1-(OH2)	2.31	2.50 ± 0.03	1.89 ± 0.03
Metal Wat2-(OH2)	3.90	4.00 ± 0.04	3.59 ± 0.04
Wat1-(OH2) Wat2-(OH2)	3.20	2.95 ± 0.05	3.53 ± 0.05
Wat1-(OH2) Glu144-(OE2)	2.67	2.48 ± 0.06	3.00 ± 0.07

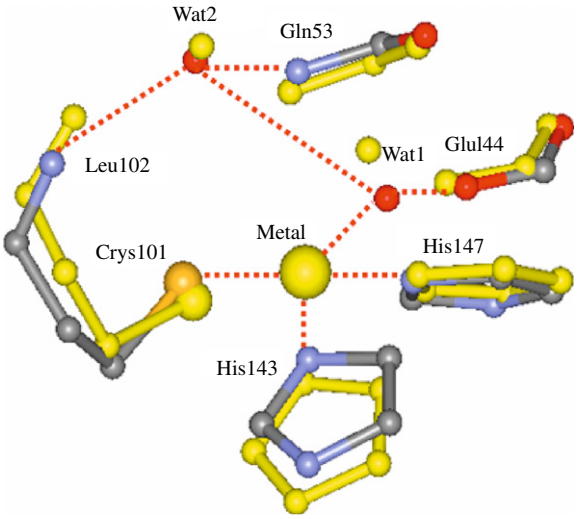

Fig. 3. Comparison between the local structure of the best fit of Co-*Li*PDF (colored stick) and Zn-*Li*PDF (thick yellow sticks) at pH9.0. The coordination of the metal ion is indicated in red dash line. (For interpretation of the references to color in this figure legend, the reader is referred to the web version of this article.)

varies between 1.80 and 2.63 Å. So we think the length of the Co-wat1 bond and Zn-wat1 bond in our measurement are reasonable. This stronger water-bonding of cobalt inhibits the transition from the tetrahedral to a five-coordinate metal center in the catalytic process and makes the distance between water and Glu144 (wat1-Glu144) become longer. In the catalytic process of PDF proteins, the very important step is that the proton of wat1 transfer to the amide at the N-terminus of the peptide with the help of Glu144 and the added positive charge makes the nitrogen suitable as a leaving group [9]. Therefore, lengthening of the wat1-Glu144 distance weakens the polarization ability of Glu144 to wat1, resulting in the proton of wat1 hardly transfer into the amide at the N-terminus.

4. Conclusion

In this work we have investigated metal-dependent enzymatic activity of the peptide deformylase from *Leptospira interrogans* (PDB code 1Y6H) by using XANES spectroscopy combining with *ab initio* multiple scattering calculations. All features in the near-edge region of the XAS spectra at the Zn and Co *K*-edge have been successfully reproduced and detailed structural information around the metal ion has been obtained. The result shows that cobalt ion presents the stronger water-bonding than zinc ion in *Li*PDF proteins. It weakens the polarization ability of Glu144 to wat1, resulting in the proton of wat1 hardly transfer to the amide at the N-terminus. It is the reason that the enzymatic activity of Co-*Li*PDF is much lower than that of Zn-*Li*PDF.

Acknowledgements

This work was partly supported by the Knowledge Innovation Program of the Chinese Academy of Sciences (KJCX2-YW-N42), the Key Important Project of the National Natural Science Foundation of China (10734070), the National Natural Science

Foundation of China (NSFC 10805055 and 10905067) and the National Basic Research Program of China (2009CB930804).

References

[1] T. Meinnel, Y. Mechulam, S. Blanquet, Biochimie 75 (1993) 1061.
[2] J.M. Adams, J. Mol. Biol. 33 (1968) 571.
[3] L.A. Ball, P. Kaesberg, J. Mol. Biol. 79 (1973) 531.
[4] D.M. Livingston, P. Leder, Biochemistry 8 (1969) 435.
[5] D. Mazel, S. Pocher, P. Marliere, EMBO J. 13 (1994) 914.
[6] P.T.R. Rajagopalan, X.C. Yu, D. Pei, J. Am. Chem. Soc. 119 (1997) 12418.
[7] Y. Li, S. Ren, W. Gong, Acta Cryst. D 58 (2002) 846.
[8] Z. Zhou, X. Song, W. Gong, J. Biol. Chem. 280 (2005) 42391.
[9] A. Becker, L. Schlichtin, W. Kabsch, D. Groche, S. Schultz, A.F. Volker Wagner, et al., Nat. Struct. Biol. 5 (1998) 1053.
[10] K. Hayakawa, K. Hatada, P. D'Angelo, S. Della Longa, C.R. Natoli, M. Benfatto, J. Am. Chem. Soc. 126 (2004) 15618.
[11] Z.Y. Wu, Y. Tao, M. Benfatto, D.C. Xian, J.Z. Jiang, J. Synchrotron Radiat. 12 (2005) 98.
[12] E. Nordlander, S.C. Lee, W. Cen, Z.Y. Wu, C.R. Natoli, A. Di Cicco, A. Filipponi, B. Hedman, K.O. Hodgson, R.H. Holm, J. Am. Chem. Soc. 115 (1993) 5549.
[13] S.D. Conradson, B.K. Burgess, W.E. Newton, A. Di Cicco, A. Filipponi, Z.Y. Wu, C.R. Natoli, B. Hedman, K.O. Hodgson, Proc. Natl. Acad. Sci. 91 (1994) 1290.
[14] K.L. Stone, R.K. Behan, M.T. Green, Proc. Natl. Acad. Sci. 102 (2005) 16563.
[15] J.J. Rehr, R.C. Albers, Rev. Mod. Phys. 72 (2000) 621.
[16] D. Groche, A. Becker, I. Schlichting, W. Kabsch, S. Schultz, A.F. Wagner, Biochem. Biophys. Res. Commun. 246 (1998) 342.
[17] M. Benfatto, A. Congiu-Castellano, A. Daniele, S. Della Longa, J. Synchrotron Radiat. 8 (2001) 267.
[18] M. Benfatto, S. Della Longa, J. Synchrotron Radiat. 8 (2001) 1087.
[19] S.D. Longa, A. Arcovito, M. Girasole, J.L. Hazemann, M. Benfatto, Phys. Rev. Lett. 87 (2001) 155501.
[20] M. Benfatto, Z.Y. Wu, Nucl. Sci. Techniques 14 (2003) 9.
[21] A. Cardelli, G. Cibin, M. Benfatto, S. Della Longa, M.F. Brigatti, A. Marcelli, Phys. Chem. Miner. 30 (2003) 54.
[22] C.R. Natoli, M. Benfatto, J. Phys. (Paris) Colloq. 47 (1986) 11.
[23] Z.Y. Wu, G. Ouvrard, S. Lemaux, P. Moreau, P. Gressier, F. Lemoigno, J. Rouxel, Phys. Rev. Lett. 77 (1996) 2101.
[24] J.C. Fuggle, J.E. Inglesfield, Unoccupied Electronic States, Topics in Applied Physics, Springer, Berlin, 1992 appendix B, 347.
[25] M. Benfatto, S. Della Longa, C.R. Natoli, J. Synchrotron Radiat. 10 (2003) 51.
[26] O.M. Roscioni, P. D'Angelo, G. Chillemi, S.D. Longa, M. Benfatto, J.Synchrotron Radiat. 12 (2005) 75.
[27] J.G. Norman, Mol. Phys. 81 (1974) 1191.
[28] Y. Joly, Phys. Rev. B 63 (2001) 125120.
[29] Z.Y. Wu, D.C. Xian, C.R. Natoli, A. Marcelli, A. Mottana, E. Paris, Appl. Phys. Lett. 79 (2001) 1918.
[30] Z. Zhou, X. Song, Y. Li, W. Gong, J. Mol. Biol. 339 (2004) 207.
[31] X.Y. Guo, W.S. Chu, W.M. Gong, Y.H. Dong, Y.N. Xie, M. Benfatto, Z.Y. Wu, High Energy Phys. Nucl. Phys. 31 (2007) 199.